Relevance of PSInSAR Analyses at ITRF Co-location Sites

Xavier Collilieux, Zuheir Altamimi, Jingyi Chen, Clément Courde, Zheyuan Du, Thomas Furhmann, Christoph Gisinger, Thomas Gruber, Ryan Hippenstiel, Davod Poreh, Paul Rebischung, and Yudai Sato

Abstract

The PSInSAR (Persistent Scatterer Interferometric Synthetic Aperture Radar) technique allows determining deformation maps over large areas. In this paper, we investigate the applicability of PSInSAR analyses for ITRF co-location sites characterized by spatial extents varying between 20 m and 3 km. Although PSInSAR shows some limitations such as spatial resolution and sparse Persistent Scatterer distribution, this technology can be used to determine relative motion between geodetic instrumentation at sufficient spatial detail, specifically for large sites. The spatial resolution varies from 3 × 22 m [rg × az] from typical Sentinel 1A/1B products (IW mode) to 0.6 × 0.25 m [rg × az] for staring spotlight mode of TerraSAR-X/Tandem-X. As an illustration, C-band PSInSAR results derived by the European Ground Motion Service (EGMS) from Sentinel 1A/1B images have been investigated for the five largest ITRF co-location sites in Europe. Maximum relative velocity differences have been found to be smaller than 2.0 mm/yr. Moreover, as high-resolution X-band SAR images show great potential for mapping deformations at high resolution, an inventory of already available TerraSAR-X/Tandem-X images at ITRF co-location sites has been established. Based on this, five candidate sites are proposed for further PSInSAR analyses using X-band data.

Keywords

Co-location · InSAR · Local tie · Space geodetic techniques · Terrestrial Reference Frame

X. Collilieux (✉) · Z. Altamimi · P. Rebischung
Université Paris Cité, Institut de physique du globe de Paris, CNRS, IGN, Paris, France

ENSG-Géomatique, IGN, Marne-la-Vallée, France
e-mail: xavier.collilieux@ensg.eu

J. Chen
University of Texas at Austin, Department of Aerospace Engineering & Engineering Mechanics, Austin, TX, USA

C. Courde
Université Côte d'Azur, CNRS, Observatoire de la Côte d'Azur, IRD, Géoazur, Observatoire de Calern, Caussols, France

Z. Du
Geoscience Australia, School of Civil and Environmental Engineering, University of New South Wales, Sydney, NSW, Australia

T. Furhmann
Airbus Defence & Space, Munich, Germany

C. Gisinger
German Aerospace Center, Remote Sensing Technology Institute, Wessling, Germany

T. Gruber
Technical University of Munich, Department of Aerospace and Geodesy, Munich, Germany

R. Hippenstiel
National Geodetic Survey, Field Operations, Chesapeake, VA, USA

D. Poreh
Universita degli Studi di Napoli Federico II, Dipartimento di Ingegneria Elettrica e delle Tecnologie dell'Informazione, Naples, Italy

Y. Sato
Geospatial Information Authority of Japan, Ibaraki, Japan

International Association of Geodesy Symposia,
https://doi.org/10.1007/1345_2024_269,

1 Introduction

The scientific community has recognized the need for a highly accurate terrestrial reference frame (TRF) for Earth Science applications. Current determinations of the International Terrestrial Reference System are made by combining data from various space geodetic techniques, namely Satellite Laser Ranging (SLR), Very Long Baseline Interferometry (VLBI), Doppler Orbitography and Radiopositioning Integrated by satellite (DORIS), Global Navigation Satellite Systems (GNSS), and terrestrial measurements from local tie surveys at co-location sites. For most of the sites, such local tie surveys are not performed on a regular basis. Thus, the assumption of equal velocity at co-location sites or the detection of some discontinuities in position time series cannot be generally verified independently from space geodesy data.

Zerbini et al. (2007) (see their Fig. 5) have shown the first Persistent Scatterer Interferometric Synthetic Aperture Radar (PSInSAR) result, also named Persistent Scatterer Interferometry (PSI), at the Medicina co-location site (Italy). As the site is located in a rural area, too few high-quality InSAR measurement points were obtained to derive the relative velocity between the GNSS and VLBI stations. However, due to the availability of new InSAR data at many sites with extended spatial coverage and shorter satellite revisit cycle, it raises the question of whether this data could serve as a supplementary resource for local tie measurements at sites lacking frequent terrestrial surveys. This analysis motivated the creation of the study group "SG 1.2.1: Relevance of PSInSAR analyses at ITRF co-location sites" of the International Association of Geodesy (IAG) in 2020.

This paper aims at reporting the conclusions and main findings of the study group. First, the strengths and weaknesses of the PSInSAR technique for relative velocity determination at co-location sites are listed. Then, some PSInSAR results at co-location sites are reviewed based on Sentinel 1A/1B radar images. Finally, perspectives are given to process and interpret X-band SAR images in the future.

2 Strengths and Limitations

Interferometric Synthetic Aperture Radar is a technique that allows determining displacements that occurred between two SAR acquisitions along the radar Line-Of-Sight (LOS) direction. In the PSInSAR approach, a large set of radar images—acquired with similar acquisition geometries—are jointly processed to estimate surface displacements at selected high-quality pixels, the so-called Persistent Scatterers (PS) (Crosetto et al. 2016). PS pixels typically have high temporal coherence, which indicates the stability of the reflection characteristics associated with the measurement points (Kotzerke et al. 2022), but PS spatial distribution is not homogenous and often correlated with landcover types. 1D-displacement time series at image acquisition times can be derived for every PS in the LOS direction of the satellite (slant measurements). Recent satellite missions often have regular short revisit cycles (Sentinel-1 satellites revisit the same area every 6 or 12 days), and thus it is possible to monitor abrupt displacement or velocity changes with PSInSAR. Several acquisition geometries may be available, for example from descending or ascending orbits, sometimes acquired from several incidence angles. However, as SAR satellites have near-polar orbits, the sensitivity to South-North displacements is very low, and only 2D displacements (i.e. in the East-West and vertical directions) can be reconstructed from PSInSAR with sufficiently high accuracy (Fuhrmann and Garthwaite 2019). The typical precision of estimated velocities is up to 1 mm/yr (Crosetto et al. 2016; Ferretti et al. 2007). PS processing requires satellite orbit (constrained by GPS), digital elevation model (DEM) and atmospheric corrections. There are many factors that influence the quality of the results, including but not limited to quality of PS candidates, temporal/spatial baselines, phase unwrapping strategy, residual atmospheric errors, and overall data analysis strategy (software). It is worth noting that PSInSAR algorithms predominantly rely on data-driven approaches to estimate not only pixel displacements but also additional corrections such as atmospheric delays or satellite orbit errors, without requiring additional auxiliary data from other geodetic techniques, with the exception of a priori orbits. Furthermore, the technique can be used for relative measurement of deformations w.r.t. a presumably stable reference location within the image extent without the need for integration into an accurate spatial reference frame.

The main drawback of PS techniques for our application is that PSInSAR determines ground, building roof or monument motion, and not necessarily the geodetic instrument reference point displacements themselves. For example, SLR instruments are located inside a building under an open dome and may be anchored more deeply than the building to which the dome is fixed. Additionally, individual instruments, such as concrete-based VLBI monuments or GNSS pillars, may be anchored at varying depths. For this reason, it is crucial to acquire PS directly on these monuments themselves. However, the availability of PS close to geodetic stations is not guaranteed due to the pixel selection process. Fortunately, PS reflection points can be constructed by installing corner reflectors (CR) or transponders. Gruber et al. (2020, 2022) studied transponders (active devices) and reported that those are easy to install and much smaller than conventional CR. They can also observe both ascending and descending arcs but some limitations have been pointed out such as

phase center correction, radio license constraint, software adaptation and possible interference with existing geodetic infrastructure (GNSS, DORIS, SLR, VLBI). As a well-known alternative, passive CR can be installed. At least five ITRF co-location sites currently host CR: Grasse (Collilieux et al. 2022), Metsähovi, O'Higgins, Wettzell, Yarragadee (Carman 2018; Balss et al. 2018).

The spatial resolution of SAR images ranges from several tens of meters to several decimeters. As the typical size of co-location sites lies between 10 m to several kilometers, small sites require high-resolution images whereas lowest resolution could still inform on relative displacements at larger sites.

As a conclusion, PSInSAR currently does not provide a measure as reliable as regular local tie surveys for our application but the availability of images and products makes it worth investigating.

3 PSInSAR Results

3.1 Sentinel 1A/1B: Ground Motion Services

A few publicly available services provide PSInSAR results at national or continental level. Most of the products rely on the Sentinel 1A/1B mission. The spatial resolution of Sentinel 1A/1B images is about 3 × 22 m [rg × az] in Interferometric Wide swath (IW) mode and 3 × 5 m [rg × az] in StripMap mode (SM). Only four of the ITRF sites are covered by the national services known to the authors: Onsala (Swedish National Space Agency 2023); Effelsberg, Potsdam, Wettzell, (BodenBewegungsdienst Deutschland; BGR 2023). Displacement results for eight co-location sites are available over Japan from Small Baseline Subset (SBAS) InSAR analysis of ALOS-2 images (L-band) provided by Geospatial Information Authority of Japan (2023) but the pixel size is about 100 m and the resolution is not sufficient for our application.

We studied European Ground Motion Service (EGMS; Copernicus 2023) results for the 22 covered ITRF co-location sites (three are located in oversea territories). Displacement time series and velocities spanning February 2015 to December 2021 are provided in the line of sight (LOS) of the satellite for each ascending and descending orbit. East/West and vertical motions also reconstructed from these two orbit results are not investigated here given that they require spatial interpolation of individual LOS results.

A visual inspection of Level 2B (L2b) products for those areas has been carried out using the EGMS online visualization tools. Level 2B products are georeferenced to ETRF2000 using GNSS permanent station coordinates (Kotzerke et al. 2022) but are still provided in the InSAR satellite LOS. No displacement has been clearly evidenced on the velocity maps available on the EGMS portal at any of the co-location sites. We further analyzed the velocity differences within the five largest co-location sites: Metsähovi, Potsdam, Reykjavik, Toulouse, Wettzell. Non-calibrated L2a products were analyzed. Those are constrained by InSAR measurements only, and referenced to a local reference point (Kotzerke et al. 2022). As a result, each orbit arc has to be assessed independently. As an example, Fig. 1a shows the raw L2a product relative velocities for the Wettzell site from a descending orbit. No significant motion is evidenced close to instruments in this figure.

For the five considered sites, 88% of stations have a measurement point available at a distance less than 20 m (considering all available orbits), see Table 1. Note that the absolute 3D position accuracy of the measurement points is less than 10 m (Kotzerke et al. 2022). Table 1 also reports the maximum relative LOS velocities w.r.t. one GNSS station of the site (closest PS). Although the standard deviation of PSInSAR velocities is between 0.1 mm/yr and 0.3 mm/yr, maximum velocity differences can be as large as 3.5 mm/yr. We note that some of the selected PS show a rather low temporal coherence. If a coherence threshold of 0.8 is chosen to filter the PS, the average number of available PS in the vicinity of the stations drops to 48%. But the velocity consistency increases, as indicated in Table 1, with maximum velocity differences of 1.4 mm/yr in Toulouse and 1.7 mm/yr in Wettzell. (The Reykjavik site is discussed in Sect. 3.2). However, the velocities of these specific PS are found to be inconsistent with the velocities of the closest high coherence PS. This example shows that the selection of relevant PS around a geodetic instrument is an important step when relating the PS-derived displacements to a potential movement of the geodetic instruments.

3.2 Sentinel 1A/1B: Examples

We investigated further EGMS displacement time series at Metsähovi since the site is composed of two sub-sites separated by 2.8 km. The GNSS stations of each sub-site show inconsistent seasonal displacements in the ITRF2020 input data (Altamimi et al. 2023), see Fig. 2a. The relative velocity of the GNSS stations of the two sub-sites are compared to the GNSS time series computed by the International GNSS Service (IGS) and projected in the LOS of the SAR satellite (ascending orbit). The individual seasonal signals predicted by the ITRF2020 analyses (Collilieux et al. 2023) are also shown. Unfortunately, as SAR images acquired during snow cover periods are excluded from EGMS products (Kotzerke et al. 2022), it is not possible to confirm GNSS seasonal displacements. However, the observed trend is consistent with space geodesy results.

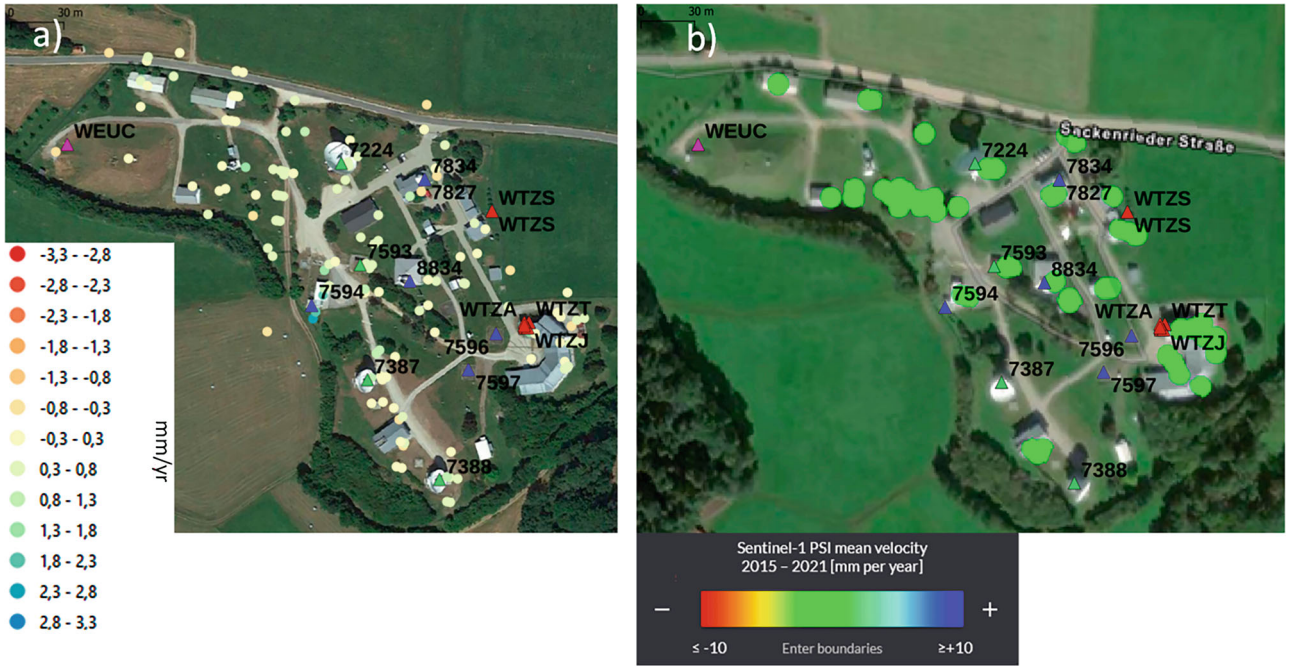

Fig. 1 PSInSAR LOS velocities at the Wettzell Observatory from two different processings of Sentinel 1A/1B data, descending orbit 095. (**a**) EGMS level 2A products, 2015/02 to 2021/12, (**b**) German ground motion service, 2015/04–2021/12. Note the different color scales in each figure. The space geodetic stations have been added as colored triangles

Table 1 Statistics on available PS at the five largest co-location sites covered by EGMS products

Site	% of stations with available PS (distance <20 m) Between brackets: only PS with temporal coherence >0.8	Max velocity differences between closest PS and the closest PS to GNSS (all orbits) (distance <20 m) Between brackets: only PS with temporal coherence >0.8, all distances
Metsähovi	81% (10%)	1.8 (0.5) mm/yr
Potsdam	94% (81%)	0.7 (0.7) mm/yr
Reykjavik	100% (67%)	1.4 (2.0) mm/yr
Toulouse	100% (100%)	0.7 (1.4) mm/yr
Wettzell	85% (44%)	3.5 (1.7) mm/yr
All 5 sites	88% (48%)	3.5 (2.0) mm/yr

As shown in Table 1, there is a significant LOS velocity difference between DORIS and GNSS at Reykjavik. Figure 2b shows the LOS relative EGMS displacements between the two DORIS sites and the Reykjavik GNSS station separated by 2.4 km. A negative trend of about −2 mm/yr is observed for the DORIS PS in the ascending orbit and is explained by displacement changes during the very last time-segment in the EGMS products. This displacement shows a clear spatial pattern. Excluding this most recent period, velocity differences from PSInSAR are small. They confirm the absence of significant motion between DORIS and GNSS stations during the ITRF2020 data period (ended in 2021.0). As an indication, the projected GNSS displacement in the satellite LOS (ascending orbit) has been computed in an absolute frame (IGS20) and reported in Fig. 2c. A velocity change is visible following the M5.6 Earthquake in February 2021 (6 km SE of Vogar, Iceland), although nothing is visible in the descending orbit (not shown). Unfortunately, the DORIS station REZB was decommissioned in September 2020, before the observed motion, so it is not possible to derive the GNSS-DORIS relative motion that could be compared to PSInSAR during this interesting period. This latter result illustrates the potential of PSInSAR results to provide a meaningful constraint for large co-location sites.

As a final remark, we compare two PSInSAR processings for the Wettzell co-location site for the same orbit arc on Fig. 1a, b. Figure 1b shows a screenshot of the German ground motion service PSInSAR result. The periods of considered data are not exactly equal but overlap significantly (see Fig. 1 caption). This figure shows that the PS distribution and LOS velocities depend on the PSInSAR algorithm. In rural locations such as the DORIS station vicinity on the left side of each figure, PS are not always detected. Specific algorithms allow getting a measurement point in this specific environment as discussed by Wang and Chen (2022), which may improve the density of detected PS in future work.

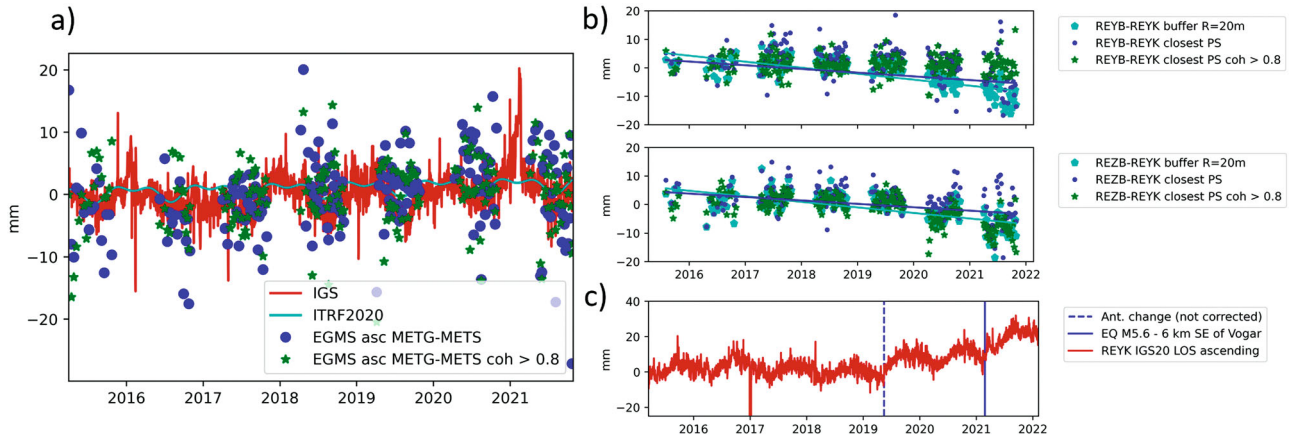

Fig. 2 (**a**) LOS displacement differences (EGMS L2a product) between the closest PS to the METG and METS GNSS stations (blue circles), same but using the closest PS with temporal coherence >0.8 (green stars), difference between GNSS station position time series from IGS projected to line of sight (red), predicted displacements from ITRF2020 input data analyses (light blue). (**b**) LOS displacement differences (EGMS L2a product) between the closest PS to the REYK (GNSS) and REYB (DORIS) stations (top) and to the REYK (GNSS) and REZB (DORIS) stations (bottom) for ascending orbit (EGMS L2a product; blue), same but using the closest PS with temporal coherence >0.8 (green), and by averaging PS displacements in 20 m radius circles (light blue). (**c**) REYK IGS station position time series (in IGS20 reference frame) projected in LOS, same orbit as **b**. The series in **c** has been detrended over the period 2013.33–2019.36 (antenna change epochs)

3.3 X-band

It is possible to derive PSInSAR results at a higher spatial resolution using SAR images from other missions. Poreh and Pirasteh (2020) studied ground deformation at the Medicina co-location site from the end of 2009 to the end of 2011 using CosmoSkyMed X-band images in StripMap/HIMAGE mode, resolution 2.5 × 2.5 m [rg × az]. At this site, a VLBI telescope and a GNSS station are installed. Unfortunately, as found by Zerbini et al. (2007) with ERS C-band SAR images, the density of obtained PS is not sufficient to study relative motion between the instruments. No PS has been found on the VLBI telescope likely due to continuous VLBI telescope motions.

Figure 3 shows X-band PSInSAR results at the Mount Stromlo site (Australia) which hosts GNSS, DORIS and SLR stations. Four years of TerraSAR-X images acquired in StripMap (SM) mode (descending orbit) spanning 26-09-2011 to 25-12-2015 have been processed using the Gamma (Werner et al. 2000) and STAMPS software packages (Hooper et al. 2012). The pixel size in this mode is about 3.5 m. All PS velocities in the displayed area show an agreement within ±1 mm/yr. It is worth noting that a PS was detected at the exact location of the STR2 pillar, but unfortunately no PS was selected at the other GNSS station STR1.

The TerraSAR-X (TSX) and TanDEM-X (TDX) missions are able to provide even higher resolutions: about 0.6 × 1.0 m [rg × az] for High Resolution SpotLight (HS) mode and about 0.6 × 0.25 m [rg × az] for Staring Spotlight (SS) mode. Figure 4a shows an amplitude image of the Yarragadee site (Australia) from SS mode which includes the VLBI (bottom

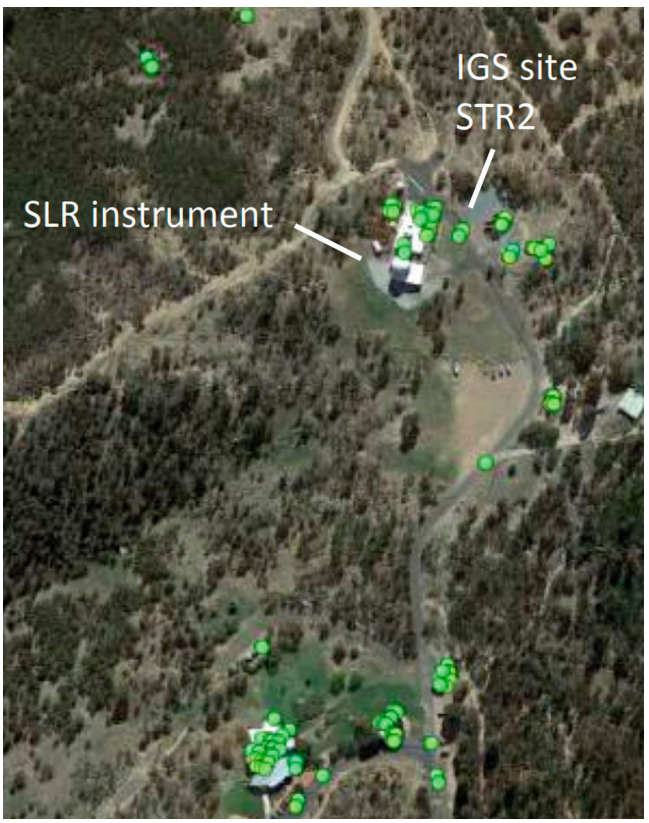

Fig. 3 PS distribution over the Mount Stromlo site (Australia) as a result of the PSInSAR analysis of TerraSAR-X images spanning 26-09-2011 to 25-12-2015 in StripMap (SM) mode

of the image) and SLR stations (top of the image). The details of the man-made infrastructure are clearly evidenced, which shows interesting perspectives to obtain a high density of

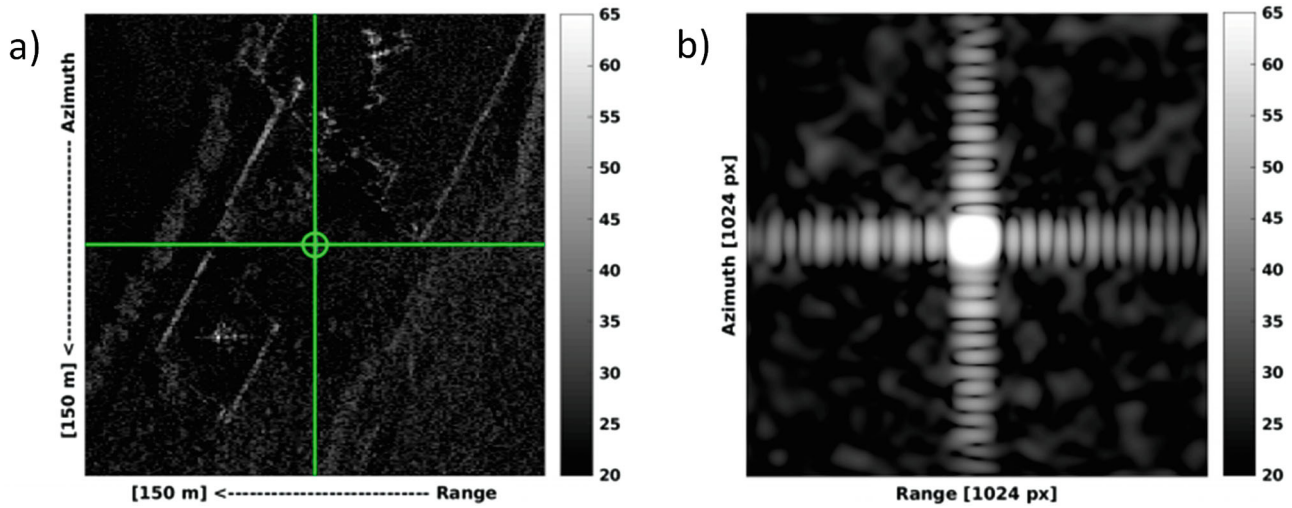

Fig. 4 (**a**) Crop of amplitude image (sigma-nought) from TerraSAR-X at Yarragadee co-location site in Staring SpotLight mode (0.6 m × 0.25 m [rg × az]). (**b**) Oversampled close up of the corner reflector (CR)

Table 2 Inventory of TDX/TSX images at ITRF co-location sites for Staring SpotLight (SS) (0.6 × 0.25 m [rg × az]) and High Resolution SpotLight (HS) (0.6 × 1.0 m [rg × az]) modes over the period 2008–2022

Site	Mode	Orbit (#)	Period
Yarragadee	SS	Ascending (147)Descending (144)	31/03/19->30/10/2208/03/19->17/12/22
	HS	Ascending (60)Descending (172)	11/03/18->21/10/1910/03/18->18/12/22
Wettzell	SS	Descending (17)	07/02/15->21/03/16
	HS	Ascending (425)Descending (205)	30/10/12->30/12/2203/04/11->01/01/23
Wuhan	SS	Descending (23)	28/06/14->15/08/17
Simeiz	SS	Ascending (13)Descending (13)	29/03/18->19/08/1801/04/18->22/08/18
O'Higgins	HS	Ascending (520)Descending (322)	05/03/08->08/12/2208/10/08->01/01/23
Metsähovi	HS	Descending (469)	12/05/13->15/12/22

PS on this site. Figure 4b shows the amplitude image of the CR that has been installed nearby and will provide a highly reliable PS with very low background scatter.

An inventory of all available TSX/TDX images at ITRF co-location sites has been developed. A web map has been developed to easily review each co-location site at https://www.arcgis.com/apps/dashboards/f9e56ed0713141c48986240faeefe684. Five co-location sites have more than 15 TSX/TDX high resolution images (SS or HS mode) available in ascending or descending arcs: Metsähovi, O'Higgins, Yarragadee, Wettzell, Wuhan. Statistics on these images are reported in Table 2. The number of candidate sites is much larger using TSX/TDX stripmap mode, resolution 2 × 3 m [rg × az].

4 Conclusion and Perspectives

This paper discussed the advantages of using PSInSAR techniques at ITRF co-location sites to supplement local tie measurements. Results obtained with Sentinel 1A/1B images were discussed and illustrated that PSInSAR is capable of providing information on relative deformation for large co-location sites. As EGMS products are updated annually, this analysis will be worth repeating regularly. Finally, X-band radar images showed a great potential for this application. A significant set of high-resolution TSX/TDX SAR images at co-location sites is already available and would gain to be processed to provide a final conclusion to this study.

Acknowledgements This study contributes to the IdEx Université de Paris ANR-18-IDEX-0001. This work is partly funded by the Centre National d'Etudes Spatiales (CNES), under TOSCA grant. Copernicus Land Monitoring Service products used in this study were produced with funding by the European Union. We are grateful to Lukas Ruesch and Amy Parker who were members of the IAG study group SG 1.2.1 (2020–2023) for fruitful discussions. We also thank the two anonymous reviewers for their relevant suggestions.

References

Altamimi Z, Rebischung P, Collilieux X, Métivier L, Chanard K (2023) ITRF2020: an augmented reference frame refining the modeling of nonlinear station motions. J Geodesy 97:47. https://doi.org/10.1007/s00190-023-01738-w

Balss U, Gisinger C, Eineder M (2018) Measurements on the absolute 2-D and 3-D localization accuracy of TerraSAR-X. Remote Sens 10:656. https://doi.org/10.3390/rs10040656

BGR (2023) BGR - BodenBewegungsdienst Deutschland, Bundesanstalt für Geowissenschaften und Rohstoffe, available at https://bodenbewegungsdienst.bgr.de, visited in June 2023

Carman R (2018) Status and recent upgrades at Yarragadee / MOBLAS-5, poster presented at 21st International Workshop on Laser Ranging Canberra

Collilieux X, Courde C, Fruneau B, Aimar M, Schmidt G, Delprat I, Defresne M-A, Pesce D, Bergerault F, Wöppelmann G (2022) Validation of a Corner Reflector installation at Côte d'Azur multi-technique geodetic Observatory. Adv Space Res 70(2):360–370. https://doi.org/10.1016/j.asr.2022.04.050

Collilieux X, Altamimi Z, Rebischung P, de la Serve M, Métivier L, Chanard K, Boy J-P (2023) A review of space geodetic technique seasonal displacements based on ITRF2020 results, REFAG 2022 proceedings, International Association of Geodesy Symposia

Copernicus (2023) Copernicus Land Monitoring Service, available at https://land.copernicus.eu/, visited in June 2023

Crosetto M, Monserrat O, Cuevas-González M, Devanthéry N, Crippa B (2016) Persistent scatterer interferometry: a review. ISPRS J Photogramm Remote Sens 115:78–89

Ferretti A et al (2007) Submillimeter accuracy of InSAR time series: experimental validation. IEEE Trans Geosci Remote Sens 45(5):1142–1153. https://doi.org/10.1109/TGRS.2007.894440

Fuhrmann T, Garthwaite M (2019) Resolving three-dimensional surface motion with InSAR: constraints from multi-geometry data fusion. Remote Sens 11(3):241. https://doi.org/10.3390/rs11030241

Geospatial Information Authority of Japan (2023) InSAR map server, available at https://maps.gsi.go.jp/#5/37.387617/138.735352/&base=english&ls=english%7Curgent_sbas_japan_merge_qu_u16&blend=0&disp=11&lcd=urgent_sbas_japan_merge_qu_u16&vs=c0g1j0h0k0l0u0t0z0r0s0m0f1&d=m, visited in June 2023

Gruber T et al (2020) Geodetic SAR for height system unification and sea level research—observation concept and preliminary results in the Baltic Sea. Remote Sens 12:3747. https://doi.org/10.3390/rs12223747

Gruber T et al (2022) Geodetic SAR for height system unification and sea level research—results in the Baltic Sea Test Network. Remote Sens 14:3250. https://doi.org/10.3390/rs14143250

Hooper A, Bekaert D, Spaans K, Arikan M (2012) Recent advances in SAR interferometry time series analysis for measuring crustal deformation. Tectonophysics 514–517:1–13. https://doi.org/10.1016/j.tecto.2011.10.013

Kotzerke P, Siegmund R, Langenwalter J (2022) End-to-end implementation and operation of the European Ground Motion Service (EGMS), Product User Manual, v1.6, EGMS-D4-PUM-SC1-2.0-007

Poreh D, Pirasteh S (2020) InSAR observations and analysis of the Medicina Geodetic Observatory and CosmoSkyMed images. Nat Hazards 103(3):3145–3161

Swedish National Space Agency (2023) InSAR Sweden, available at http://insar.rymdstyrelsen.se/, visited in June 2023

Wang K, Chen J (2022) Accurate persistent scatterer identification based on phase similarity of radar pixels. IEEE Trans Geosci Remote Sens 60(1–13):5118513. https://doi.org/10.1109/TGRS.2022.3210868

Werner C, Wegmüller U, Strozzi T, Wiesmann A (2000) GAMMA SAR and interferometric processing software. In European Space Agency, (Special Publication) ESA SP. 461, 211–219

Zerbini S, Richter B, Rocca F, van Dam T, Matonti F (2007) A combination of space and terrestrial geodetic techniques to monitor land subsidence: case study, the southeastern Po Plain, Italy. J Geophys Res 112:B05401. https://doi.org/10.1029/2006JB004338